Anomalous behavior of normal kinematic restitution in the oblique impacts of a hard sphere on an elasto-plastic plate

Michel Y. Louge and Michael E. Adams
Sibley School of Mechanical and Aerospace Engineering, Cornell University, Ithaca, NY
(July 30, 2001)

We observe oblique impacts of a hard aluminum oxide sphere on a thick elasto-plastic polycarbonate plate by recording stroboscopic photographs of the sphere trajectory and spin. The apparent kinematic coefficient of normal restitution grows monotonically with the magnitude of the tangent of the angle of incidence, and the apparent coefficient of friction decreases with increasing normal impact velocity. Although every collision dissipates the total kinetic energy of the sphere, we observe restitution coefficients exceeding unity for the most grazing impacts. We exploit this example to confirm that, although an apparent kinematic coefficient of normal restitution below one is sufficient to guarantee dissipation of kinetic energy in any collision, this condition is not necessary for oblique impacts of spheres on a plate.

81.70.Bt,62.20.Fe,62.20.Dc,46.55.+d

I. INTRODUCTION

Theories [1] and numerical simulations [2] for collisional flows of granular materials predicate their success on modeling the impacts of individual grains accurately. To make these theories tractable, individual collisions are described using the simplified treatment that Walton proposed [3]. Walton ignores the detailed dynamics of each impact. Instead, he predicts the collision outcome using three constant parameters. Experiments have shown that this simple model adequately describes binary impacts of spheres [4,5] and slightly aspherical particles [6], as well as impacts of spheres of various materials on flat plates [4–7]. Discrete Element Simulations incorporating this model have successfully reproduced actual collisional flows carried out in microgravity [8].

One of the three parameters in Walton's model is a kinematic coefficient of normal restitution. The conventional assumption is that it is less than one. However, as this paper will show, there are peculiar instances in which this coefficient exceeds unity for oblique impacts. We begin with a summary of the model and its limitations. We then describe the apparatus briefly and discuss the significance of our experimental observations.

II. BACKGROUND

To describe the impact of a sphere on another sphere or a stationary wall, Walton invokes three assumptions [3]. First, the contact area between the impact protagonists reduces to a single point through which all forces are exerted. Second, rather than modeling the time-history of these forces, Walton focuses instead on the total collisional impulse $\mathbf{J}$, which represents their integral over the entire collision time. Third, Walton closes his model using three constant parameters to be determined experimentally [4–7]. What follows is a summary of the corresponding analysis for a sphere impacting a stationary half-space.

Consider a rigid sphere of diameter d, center of mass velocity $\mathbf{c}$ and spin ω before impact (Fig. 1). The relative velocity of the contact point is

$$\mathbf{u} = \mathbf{c} - (d/2)\omega \times \mathbf{n}, \tag{1}$$

where $\mathbf{n}$ is the unit normal vector perpendicular to the plate. The incident angle γ between $\mathbf{u}$ and $\mathbf{n}$ characterizes the impact geometry, $\cot\gamma \equiv \mathbf{u}\cdot\mathbf{n}/|\mathbf{u}\times\mathbf{n}|$. Because impacts occur when $\mathbf{u}\cdot\mathbf{n} \le 0$, this angle lies in the range $\pi/2 \le \gamma \le \pi$.

The post-collision velocities are derived by writing the balance of linear and angular momenta in the collision and by invoking Walton's three-parameter closure. The first parameter is the kinematic coefficient of normal restitution e. It characterizes the incomplete restitution of the normal component of $\mathbf{u}$,

$$\mathbf{n}\cdot\mathbf{u}' = -e\mathbf{n}\cdot\mathbf{u} \tag{2}$$

where primes denote conditions after the collision. The existence of a rebound requires $e \ge 0$.

The conventional assumption [4] is that the kinematic coefficient of normal restitution also satisfies $e \leq 1$. In fact, as Chatterjee and Ruina [9] pointed out, although this condition is sufficient to guarantee that the model predicts dissipation of kinetic energy in the collision, it is not necessary for oblique impacts of spheres. Using thin disks levitated on an air table, Calsamiglia et al. [10] observed a single data point for which the impact on a thick plate may have exhibited a normal restitution exceeding unity. As we will illustrate with a hard sphere colliding on an elasto-plastic plate, values of $e > 1$ are indeed possible without implying kinetic energy production in the impact or, in other words, without violating the second law of thermodynamics.

Smith and Liu [11] made a similar point for certain non-colinear impacts in which the normal at the contact point is not directed along the line joining the centers of mass of the two colliding bodies. Using finite element modeling, these authors showed that the kinematic coefficient of normal restitution of the hemi-spherical ends of a circular rod impacting a half-space can exceed one. They briefly reported simple experiments in which a "superball" bonded to the end of a cylindrical rod exhibited values of e as high as 1.4.

Nonetheless, Smith [12] also showed that the condition $e < 1$ is not sufficient to uphold the second law for all possible frictional, non-colinear impacts of non-spherical bodies. To avoid such violation, Wang and Mason [13] and Stronge [14,15] proposed alternative definitions of restitution. The first defines normal restitution as the ratio of impulses during the compression and restitution phases of the impact [13]. The other equates the square of the normal restitution coefficient to the ratio of the elastic strain energy released during restitution to that absorbed during compression [14,15]. However, because these definitions are difficult to implement in the kinetic theory of collisional granular materials or in the corresponding Discrete Element Simulations, the kinematic closure in Eq. (2) is generally preferred, particularly if all grains are spherical.

The second parameter in Walton's model arises when grazing collisions with incident angles near $\pi/2$ involve gross sliding. For these, Walton assumes that sliding is resisted by Coulomb friction and that the tangential and normal components of the impulse $\mathbf{J}$ are related by the coefficient of friction μ,

$$|\mathbf{n} \times \mathbf{J}| = \mu(\mathbf{n} \cdot \mathbf{J}), \tag{3}$$

where $\mu \geq 0$.

For greater values of the incident angle, the impact is closer to head-on and it no longer involves gross sliding as parts of the contact patch are brought to rest. When γ exceeds the limiting angle γ_0, Walton replaces Eq. (3) with

$$\mathbf{n} \times \mathbf{u}' = -\beta_0 \mathbf{n} \times \mathbf{u}, \tag{4}$$

where $\gamma_0 \equiv \pi - \arctan[7(1+e)\mu/2(1+\beta_0)]$ and β_0 is the tangential coefficient of restitution. For simplicity, he then categorizes the collision as "sticking" and assumes that the entire contact point is brought to rest during impact. For sticking collisions, the definition of β_0 in Eq. (4) implies that some of the elastic strain energy stored in the solid during impact is recoverable through tangential compliance, so the tangential velocity of the point of contact may be reversed. In Walton's model, Eqs. (3) and (4) are mutually exclusive i.e., the point of contact is either sliding (Eq. 3) or sticking (Eq. 4). This exclusion thus distinguishes two separate impact regimes. Walton also assumes that β_0 is constant and satisfies $0 \leq \beta_0 \leq 1$.

In fact, β_0 varies with the angle of incidence [4–7,16,17], starting with negative values for nearly head-on collisions, and becoming positive throughout the rest of the sticking regime. In principle, β_0 can also exceed unity, as long as this does not imply the creation of kinetic energy in the impact. Because typical spheres engaged in a collisional granular flow experience few contacts with $\gamma > \gamma_0$, the crudeness of Eq. (4) seldom matters in practice [18].

A convenient way to interpret data from an impact experiment is to follow Maw, Barber and Fawcett [16,17] and produce a plot of $\Psi_2 \equiv -(\mathbf{u}' \cdot \mathbf{t})/(\mathbf{u} \cdot \mathbf{n})$ versus $\Psi_1 \equiv -(\mathbf{u} \cdot \mathbf{t})/(\mathbf{u} \cdot \mathbf{n})$, where $\mathbf{t}$ is a unit vector located in the collision plane $(\mathbf{u}, \mathbf{n})$ and parallel to the plate. In collisions of a homogeneous sphere that involves gross sliding,

$$\Psi_2 = \Psi_1 - \frac{7}{2}(1+e)\mu \, sign(\mathbf{u} \cdot \mathbf{t}); \tag{5}$$

and in collisions that do not,

$$\Psi_2 = -\beta_0 \Psi_1. \tag{6}$$

Foerster et al. [4] provide a detailed derivation of these Eqs. For positive values of $\mathbf{u} \cdot \mathbf{t}$, Ψ_1 represents the magnitude of the tangent of the incident angle. Similarly, the ratio (Ψ_2/e) is the tangent of the rebound angle γ' between $\mathbf{n}$ and $\mathbf{u}'$. If the coefficients e, μ and β_0 are constant, data plotted as Ψ_2 versus Ψ_1 fall on two distinct straight lines Eqs.(5) and (6) that permit unambiguous identification of the sliding and sticking regimes. This paper reports a case where such a plot must be complemented by a detailed look at the dependence of e on Ψ_1 and of μ on normal impact velocity.

III. APPARATUS

The experimental apparatus is derived from that of Foerster et al. [4]. A solenoid valve connected to a vacuum pump releases a 99.5% alumina ceramic sphere of diameter $3.175\,mm$ and density $3.87\,g/cm^3$ (Hoover Precision) in a free fall without spin above a thick and wide polycarbonate plate of Lexan.

A computer running the LabView software coordinates the release of the sphere and the image acquisition from a Pulnix TM1010 digital CCD camera with 1024×1024 square pixels of $9\,mm$ width. Stroboscopic illumination allows the camera to record successive positions of the sphere before and after the collision through a TAMRON 23FM25L lens of $25\,mm$ focal length and $F/1.6$ to 16 (Fig. 2). The digitized pictures are analyzed using computer vision software. A circle is superimposed upon each sphere image to establish the location of its center. Because the collision has a very short duration, it cannot be observed. Instead, the position and velocity of the sphere at impact are extrapolated from two successive images on the photograph. From this extrapolation, we infer the unit normal $\mathbf{n}$ and the linear velocities $\mathbf{c}$ and $\mathbf{c}'$ before and after impact. This permits us to evaluate the collisional impulse

$$\mathbf{J} = m(\mathbf{c}' - \mathbf{c}), \tag{7}$$

where m is the mass of the sphere.

We also record the spin ω' after impact by tracking the angular position of a mark drawn on the white sphere (Fig. 2). As Fig. 3 indicates, this observation agrees well with the value of ω' that is independently calculated from the measured impulse, assuming that all forces are exerted at a single contact point,

$$I(\omega' - \omega) = -(d/2)\mathbf{n} \times \mathbf{J}, \tag{8}$$

where $I = md^2/10$ is the moment of inertia about the center of the homogeneous sphere and, because this apparatus releases the sphere without initial spin, $\omega = \mathbf{0}$.

From known linear and angular velocities, we then calculate the relative velocities at contact $\mathbf{u}$ and $\mathbf{u}'$ and plot the corresponding values of Ψ_2 and Ψ_1. Foerster et al. provide further details of the experimental apparatus and data analysis [4].

IV. RESULTS AND DISCUSSION

The data in Fig. 4 clearly reveals two impact regimes. For $\Psi_1 > \Psi_0 = 1.5 \pm 0.2$, oblique collisions appear to conform to Eq. (5) with gross sliding. Below this value, Eq. (6) adequately represents the relation between γ and γ' for nearly head-on collisions with $\beta_0 = 0.26 \pm 0.05$.

However, as Fig. 5 shows, the apparent values of normal restitution increase with Ψ_1. The growth is well represented by the empirical relation

$$e = e_0 + (1 - e_0)\Psi_1/\Psi_t, \tag{9}$$

where $e_0 = 0.91$ is the restitution for head-on collisions. Remarkably, normal restitution clearly exceeds unity for $\Psi_1 > \Psi_t = 3.7$. As Fig. 6 indicates, this does not imply that the sphere rebounds with greater kinetic energy than what it possessed before impact.

In fact, the kinematic normal restitution of a sphere on a half-space can exceed unity, even though the total kinetic energy is dissipated in the collision. To show this, we first evaluate the ratios of the kinetic energies of translation T' and rotation R' after impact to the total kinetic energy K before impact. Denoting the sticking and sliding regimes with the subscripts β and μ, respectively, these ratios are

$$\frac{T'_\beta}{K} = \frac{1}{(1 + \Psi_1^2)}[e^2 + \frac{1}{49}(5 - 2\beta_0)^2\Psi_1^2], \tag{10}$$

$$\frac{R'_\beta}{K} = \frac{1}{(1 + \Psi_1^2)}\frac{10}{49}(1 + \beta_0)^2\Psi_1^2, \tag{11}$$

in the sticking regime, and

$$\frac{T'_\mu}{K} = \frac{1}{(1 + \Psi_1^2)}(e^2 + [\mu(1 + e) - \Psi_1]^2), \tag{12}$$

$$\frac{R'_\mu}{K} = \frac{1}{(1+\Psi_1^2)}\frac{5}{2}\mu^2(1+e)^2, \tag{13}$$

in the sliding regime. A necessary and sufficient condition for total kinetic energy dissipation is $(T' + R') < K$ or, equivalently,

$$(1-\beta_0^2)\Psi_1^2 > -(7/2)(1-e^2) \tag{14}$$

in the sticking regime and

$$\Psi_1 > \Psi_c \equiv \frac{7}{4}\mu(1+e) - \frac{1-e}{2\mu} \tag{15}$$

in the sliding regime. In Walton's model, the boundary between the two regimes occurs where

$$\Psi_1 = \Psi_0 \equiv \frac{7}{2}\mu(\frac{1+e}{1+\beta_0}). \tag{16}$$

Thus, if $0 \leq \beta_0 \leq 1$, requiring $e \leq 1$ is sufficient to uphold Eq. (14) in the sticking regime and, because $\Psi_0 > \Psi_c$, to satisfy Eq. (15) in the sliding regime as well. For head-on collisions with $\Psi_1 = 0$, the condition $e \leq 1$ is also necessary (Eq. 14). Thus, if the normal restitution conforms to Eq. (9), the latter must satisfy $e_0 \leq 1$.

However, for oblique impacts, $e \leq 1$ is not a necessary condition. To illustrate this point, let us assume that normal restitution grows according to Eq. (9) and that the friction coefficient is roughly constant. Let us then focus on values of $\Psi_1 > \Psi_t$ for which $e > 1$. Without much loss of generality, let us also assume that normal restitution may only exceed one in the sliding regime i.e., $\Psi_t > \Psi_0$. Algebraic manipulations of Eqs. (9) and (15) yield a necessary and sufficient condition that e_0, μ and Ψ_t must satisfy to guarantee the dissipation of total energy in impacts at any $\Psi_1 > \Psi_t$,

$$\Psi_t > \max\left[(1-e_0)(\frac{1}{2\mu} + \frac{7}{4}\mu), \frac{7}{2}\mu\right]. \tag{17}$$

Thus, if condition (17) is upheld, the apparent kinematic coefficient of normal restitution can in principle grow *ad infinitum* through Eq. (9) without violating the second law. Chatterjee and Ruina discuss this paradox further for bodies of arbitrary geometry [9].

Our observations suggest a subtle coupling between the normal and tangential contact forces in the impact. Note that, because our experiments do not resolve the detailed dynamics of the collision, they only yield apparent values of normal restitution and friction that are based upon the fixed normal $\mathbf{n}$ to the whole plate. However, as Larsson and Storåkers showed [19], the oblique indentation of a hard solid on a softer half-space leads to asymmetric deformations of the latter. Then, on the microscopic scale, the normal $\mathbf{n}$ may not remain a meaningful measure of the relative orientation of the contact surfaces throughout the duration of oblique collisions.

Instead, the gradual increase of the apparent restitution with $\Psi_1 = |\tan\gamma|$ may be associated with a small rotation of the effective normal, which could arise from local deformations of the plate's surface. If the latter rotated toward the incoming sphere by an angle α, the restitution and friction based on $\mathbf{n}$ would appear, in the sliding regime, as

$$e = [(e' - \mu\tan\alpha) + (1+e')\Psi_1\tan\alpha]/(1+\mu\tan\alpha) \tag{18}$$

and

$$\mu = (\mu' + \tan\alpha)/(1-\mu'\tan\alpha), \tag{19}$$

where e' and μ' are the values of restitution and friction based on the new local orientation. Because $\mu'\tan\alpha$ and $\tan\alpha \ll 1$, Eqs. (18) and (19) reduce approximately to $\mu' \sim \mu$ and $e \sim e' + (1+e')\Psi_1\tan\alpha$. Comparing this expression with the empirical fit in Eq. (9) suggests that a typical local surface rotation, if it exists, is on the order of $\alpha \sim 0.8°$. Because we measure the relative orientation of $\mathbf{n}$ and $\mathbf{u}$ to a precision better than $0.1°$, the increase in e that we observe cannot arise from a systematic error in our measurement of γ, and therefore it is not an artifact of our experiments.

Finally, the normal restitution is likely to depend upon normal impact velocity. Several authors have proposed theories predicting variations of e with $|\mathbf{u}\cdot\mathbf{n}|$ for elasto-plastic spheres [20–24]. Gorham and Kharaz [7] recently conducted careful experiments showing a substantial dependence of e on $|\mathbf{u}\cdot\mathbf{n}|$ for both head-on and oblique collisions of aluminum oxide spheres on an aluminum plate. Unfortunately, in our apparatus and theirs, the normal velocity

is equally affected by the plate inclination, which determines the impact geometry through Ψ_1, and by the release height h, which sets the velocity magnitude,

$$|\mathbf{u}\cdot\mathbf{n}| = \sqrt{2gh}/\sqrt{1+\Psi_1^2}, \tag{20}$$

where $g = 9.81 m/s^2$ is the acceleration of gravity.

In an attempt to distinguish the role of the impact geometry and that of the normal velocity, we released the sphere from two possible heights $h = 12$ or $25\,cm$ above the plate. As Fig. 5 shows, the data sets of e versus Ψ_1 corresponding to the two magnitudes of $|\mathbf{u}|$ are indistinguishable within experimental error. In contrast, data from the two heights collapse less well on a graph of e versus $|\mathbf{u}\cdot\mathbf{n}|$ (Fig. 7). In fact, the data is reasonably captured by an expression combining Eqs. (9) and (20). Thus, it is unlikely that variations of e can be solely attributed to a dependence on $|\mathbf{u}\cdot\mathbf{n}|$.

When the contacts are in gross slip, we observe that the apparent friction decreases with increasing normal impact velocity $|\mathbf{u}\cdot\mathbf{n}|$ (Fig. 8), thus supporting the conjecture of Gorham and Kharaz [7]. The data can be fitted using

$$\mu = \mu_d + (\mu_s - \mu_d) exp(-|\mathbf{u}\cdot\mathbf{n}|/v_c) \tag{21}$$

with $\mu_s = 0.45$, $\mu_d = 0.05$ and $v_c = 1.4\,m/s$. In contrast, the friction data do not correlate well with $|\mathbf{u}\cdot\mathbf{t}|$ alone (Fig. 9), or with Ψ_1 alone (Fig. 10).

V. CONCLUSIONS

Experiments with hard ceramic spheres impacting a softer polycarbonate plate have confirmed the hypothesis of Chatterjee and Ruina [9] that the apparent kinematic coefficient of normal restitution can exceed one without artificially creating kinetic energy in the collision. These results call into question theories for spheres impacting an elasto-plastic half-space, which assume that $e \leq 1$. Despite this anomaly, Walton's simple impact closure remains useful when it is supplemented by empirical relations capturing the dependence of the apparent normal restitution on the incident angle and that of the apparent friction coefficient on the normal impact velocity.

VI. ACKNOWLEDGMENTS

The authors are indebted to Colin Thornton, Alexandre Valance and Luc Oger for useful suggestions. They are grateful to Amelia Dudley, Siddharth Sinha, Priscilla Carreon and Musyoka Munyoki for helping with the experiments, to Reno Giordano, James Buckley and Peter Weisz for designing the computer control of the experiment and its image capture, and to Arvind Gopinath for helping with REVTeX. This work was supported by NASA grants NCC3-468 and NAG3-2112.

---

[1] J.T. Jenkins, in *Research Trends in Fluid Mechanics* (Lumley, J.L., et al., eds.), AIP Press, Woodbury, NJ (1996).
[2] M.A. Hopkins and M. Louge, *Phys. Fluids A* **3**, 47-57 (1991).
[3] O.R. Walton, in *Particulate Two-Phase Flow*, M.C. Roco, ed., Butterworth-Heinemann (1993), p. 884-907.
[4] S.F. Foerster, M.Y. Louge, H. Chang and K. Allia, *Phys. Fluids* **6**, 1108-1115 (1994).
[5] L. Labous, A.D. Rosato and R.N. Dave, *Phys. Rev. E* **56**, 5717-5725 (1997).
[6] A. Lorenz, C. Tuozzolo and M.Y. Louge, *Experimental Mechanics* **37**, 292-298 (1997).
[7] D.A. Gorham and A.H. Kharaz, *Powder Tech.* **112**, 193-202 (2000).
[8] M.Y. Louge, J.T. Jenkins, H. Xu and B. Arnarson, in the *Proceedings of ICTAM-2000*, H. Aref and J.W. Phillips, eds., Kluver Academic Publishers, Boston (2001), in press.
[9] A. Chatterjee and A. Ruina, *J. Applied Mech.* **65**, 939-951 (1998).
[10] J. Calsamiglia, S.W. Kennedy, A. Chatterjee, A. Ruina and J.T. Jenkins, *J. Appl. Mech.* **66**, 146-152 (1999).
[11] C.E. Smith and P.-P. Liu, *J. Appl. Mech.* **59**, 963-969 (1992).
[12] C.E. Smith, *J. Appl. Mech.* **58**, 754-758 (1991).
[13] Y. Wang and M.T. Mason, *J. Appl. Mech.* **59**, 635-642 (1992).

[14] W.J. Stronge, *Proc. Roy. Soc. Lond. A* **431**, 169-181 (1990).
[15] W.J. Stronge, *Int. J. Impact Engng.* **15**, 435-450 (1994).
[16] N. Maw, J.R. Barber and J.N. Fawcett, *Wear* **38**, 101-114 (1976).
[17] N. Maw, J.R. Barber and J.N. Fawcett, *ASME J. of Lubrication Technology* **103**, 74-80 (1981).
[18] M.Y. Louge, *Phys. Fluids* **6**, 2253-2269 (1994).
[19] J. Larsson and B. Storåkers, *Eur. J. Mech. A/Solids* **19**, 565-584 (2000).
[20] W. Goldsmith, *Impact - The Theory and Behaviour of Colliding Solids*, Edward Arnold, London (1960).
[21] C. Thornton and Z. Ning, *Powder Tech.* **99**, 154-162 (1998).
[22] L. Vu-Quoc, X. Zhang and L. Lesburg, *J. Appl. Mech.* **67**, 363-371 (2000).
[23] N. V. Brilliantov, F. Spahn, J.M. Hertzsch and T. Pöschel, *Phys. Rev. E* **53**, 5382-5392 (1996).
[24] S.D. Mesarovic and N.A. Fleck, *Proc. Roy. Soc. Lond. A* **455**, 2707-2728 (1999).

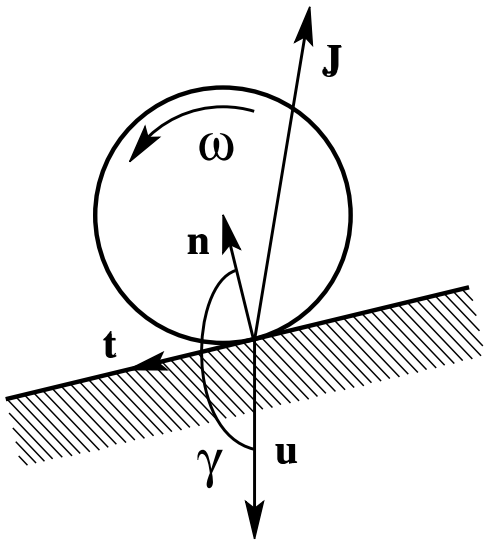

FIG. 1. Impact geometry.

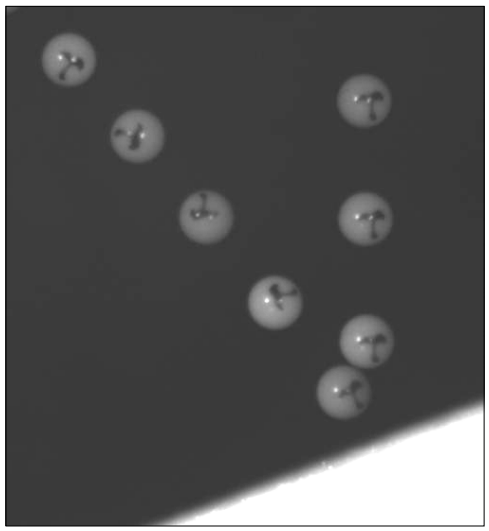

FIG. 2. Typical image with $\gamma = 160^\circ$, $\Psi_1 = 0.364$, $\Psi_2 = 0.033$, $|\mathbf{u}\cdot\mathbf{n}| = 1.4\,m/s$, $|\mathbf{u}\cdot\mathbf{t}| = 0.5\,m/s$ and $\omega' = 250\,rad/s$ at a stroboscope frequency of $200\,Hz$.

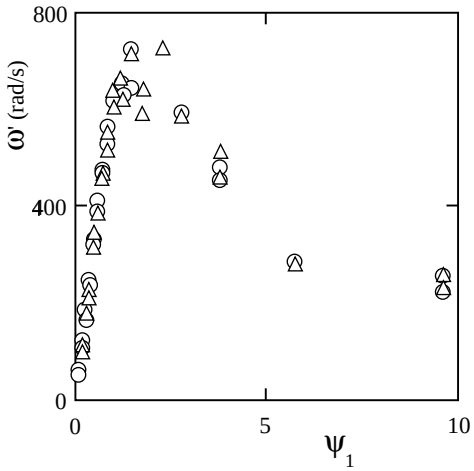

FIG. 3. Post-collision rotation rate versus Ψ_1 for $|\mathbf{u}| = 1.5\,m/s$. The triangles represent rates inferred from Eqs. 7 and 8. The circles are rates measured by tracking the rotation of marks drawn on the spheres (Fig. 2).

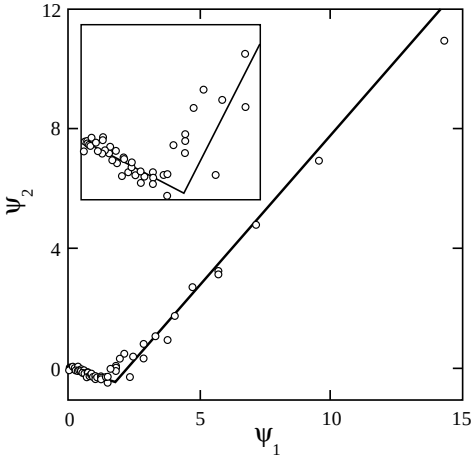

FIG. 4. Plot of Ψ_2 versus Ψ_1. The insert is a detail near the origin.

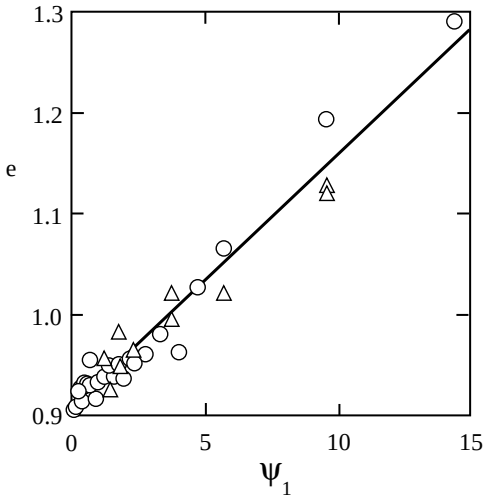

FIG. 5. Kinematic coefficient of normal restitution versus $\Psi_1 = |\tan\gamma|$. The triangles and circles are data with $|\mathbf{u}| = 1.5\,m/s$ ($h = 12\,cm$) and $|\mathbf{u}| = 2.2\,m/s$ ($h = 25\,cm$), respectively.

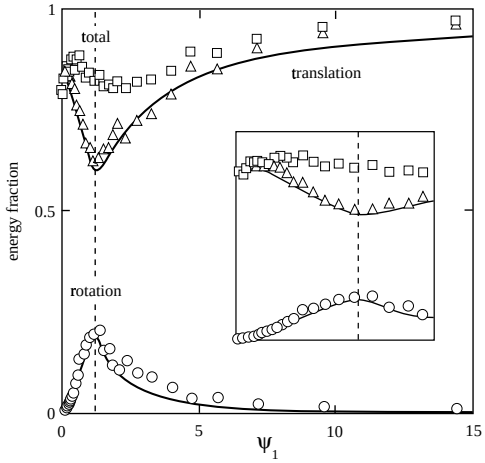

FIG. 6. Measured post-collision kinetic energies as a fraction of the total kinetic energy K before impact for experiments with $h = 25\,cm$. The circles, triangles and squares represent the rotation energy R', translation energy T' and total energy K', respectively. The curves are a model based on Eqs. (9) through (13), $\mu = 0.23$ and $\beta_0 = 0.26$. The insert shows details near $\Psi_1 = 0$. The vertical dashed line denotes the transition between the sticking and sliding regimes.

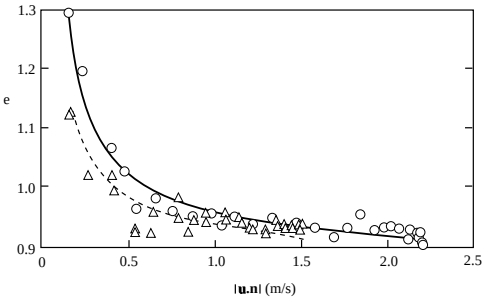

FIG. 7. Kinematic coefficient of normal restitution versus normal velocity at contact; for symbols, see Fig. 5. The solid and dashed lines represent models combining Eqs. (9) and (20) for $h = 25\,cm$ and $12\,cm$, respectively.

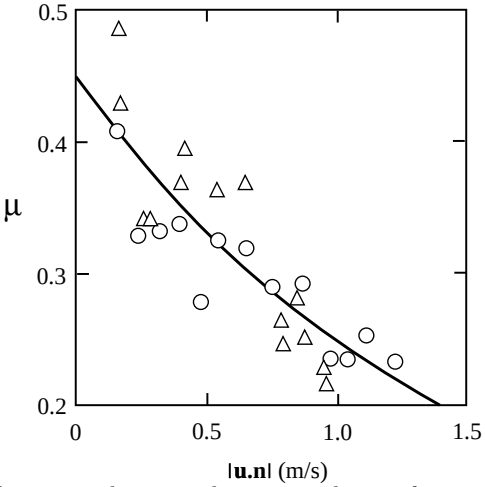

FIG. 8. Dependence of the friction coefficient on the normal impact velocity; for symbols, see Fig. 5. The solid line is the empirical fit of Eq. (21).

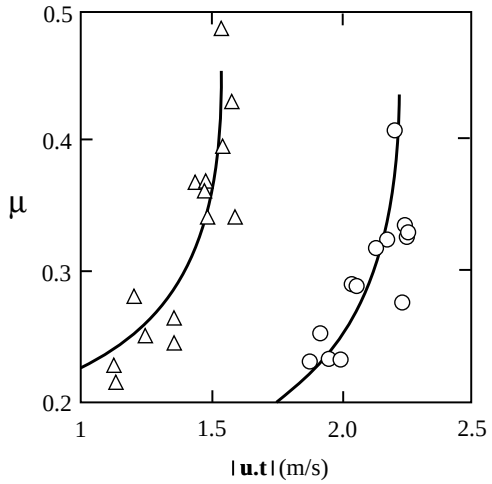

FIG. 9. Dependence of the friction coefficient on the tangential impact velocity. The solid lines are fits to the data for $|\mathbf{u}| = 1.5\,m/s$ (triangles) and $|\mathbf{u}| = 2.2\,m/s$ (circles) combining Eqs. (20) and (21).

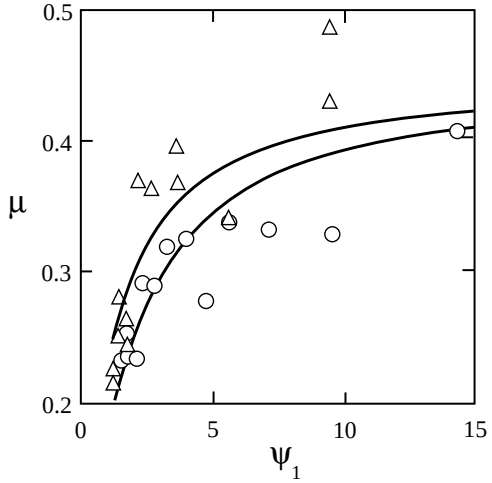

FIG. 10. Dependence of the friction coefficient on Ψ_1; for symbols and lines, see Fig. 9.